PAPER

Check for updates

Accelerated ageing of silicone rubber and XLPE used in HV cable accessories: a thermomechanical analysis

Oscar Kayanja,[a] Emre Kantar,[b] Svein M. Hellesø,[b] Julia Glaum,[a] Sverre Hvidsten[b] and Mari-Ann Einarsrud ✪ *[a]

Medium and high-voltage cable accessories, such as terminations and connectors, operate under harsh mechanical and thermal stresses, influencing long-term reliability. These stresses may lead to deterioration in the mechanical properties of the materials, thereby reducing radial pressure. Hence, the number and size of microcavities at the solid–solid interfaces will increase, being detrimental to the electrical breakdown strength. To mitigate this, applying external compressive pressure after installation is proposed to address challenges with the microcavities. However, the long-term effect of the external compressive pressure on the mechanical properties of the materials remains unclear. This study investigates the combined effect of mechanical compression and thermal cycling on two types of insulating silicone rubber (SiR) and semiconductive SiR used in HV cable accessories, comparing them with cross-linked polyethylene (XLPE). The materials were subjected to 25% compressive strain and thermal cycling between −20 and 110 °C in air, while another set underwent only thermal cycling. Ageing under compression increased the compression set by ~1% in hard SiR and ~3% in soft and semiconductive SiR compared to unaged materials. Surface hardness increased significantly in soft and semiconductive SiR (~3.7%) but slightly in hard SiR (~0.3%). Surface roughness increased by 0.7−0.9 μm across all materials. After ageing, the stress-relaxation response decreased for both hard and soft SiR, whereas semiconductive SiR showed a slight increase. The material response to cyclic loading after accelerated ageing is presented, along with the suitability of these materials for future cable termination designs.

1. Introduction

Silicone rubber (SiR) is used as an insulator in cable accessories such as joints, terminations, and connectors due to its chemical and thermal stability and insulating properties.[1–3] The service life of such cable accessories is influenced by a range of factors, including electrical insulation and stress grading material types, thermomechanical forces, insulation and overvoltage requirements, voltage rating, overall quality of components, as well as the diligence of the workmanship during installation of cable systems. The cable accessories include non-cross-linked solid–solid polymer interfaces that are reported to be electrically the weakest link in the cable systems. This is due to imperfect material surfaces, leading to microcavities of different sizes and shapes at the interface.[4] The size of the microcavities can be reduced by increasing the contact/interfacial pressure[5,6] and the application of an exter-

nal radial pressure can be an alternative to minimise the size and number of interfacial microcavities.[7] This will enhance the breakdown strength of the interface by increasing the inception voltage of electrical discharges, *i.e.*, partial discharges (PD), that can gradually lead to electrical tree formation and then an electrical breakdown.[8–10]

In addition to electrical stress, materials used in cable accessories are subjected to cyclic thermal and operational mechanical stresses. Under normal operation, the temperature may rise up to 90 °C (maximum allowed conductor temperature by IEC design criteria),[11] and under short circuit conditions, the temperature can go up to 250 °C for a very short time.[12,13] Seasonal variations and operational conditions will affect the interfacial pressure between the accessory and the cable insulation. Stress relaxation of the rubber in the accessory influenced by the thermomechanical factors may eventually result in a decline in the interfacial pressure, which in turn reduces the electrical performance of the cable accessory.[14]

A schematic of the cross-section of a cable termination is shown in Fig. 1. The outer body of a prefabricated slip-on termination (SOT) can be made of SiR seamlessly cross-linked

[a] Department of Materials Science and Engineering, NTNU Norwegian University of Science and Technology, Trondheim, Norway. E-mail: mari-ann.einarsrud@ntnu.no
[b] Electric Power Technology, SINTEF Energy Research, Trondheim, Norway

© 2026 The Author(s). Published by the Royal Society of Chemistry
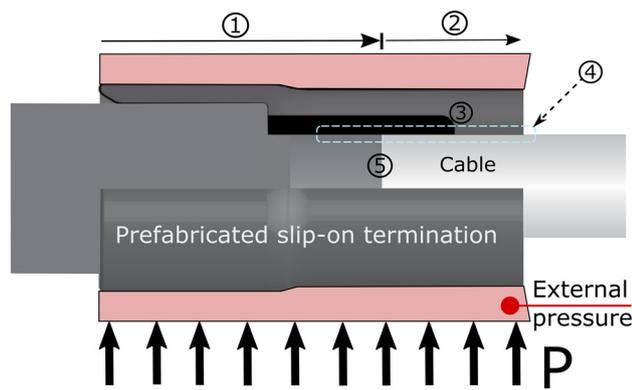
RSC Appl. Polym., 2026, **4**, 785–795 | 785

Fig. 1 Schematics of the cable-termination interface. Axial section with 1: no electrical stress outside cable/connector, 2: high electrical stress outside cable/connector. 3: Electrical field grading. 4: Interface between the SOT and cable. 5: End cut of the insulation screen of the cable. P: Uniform radial external pressure on the SOT using an external pressure unit.

with a semi-conductive material (3) (*e.g.*, SiR blended with carbon black), with a key role of geometric electric field grading at the end cut of the insulation screen (5).[15] A radial interfacial pressure is obtained from the elastic behaviour of SiR when expanded onto the cable insulation. The interface between the cable and the SOT, being the most critical section, is highlighted with a dashed box (4) in Fig. 1. SiR is in contact with the cable insulation, and material properties and compatibility at the interface are crucial for the electrical breakdown strength.

To regulate the interfacial pressure, rather than allowing it to be determined solely by the geometry of the cable, the cable accessory and the intrinsic mechanical properties of the material, we propose to include an external pressure device to the outer surface of the cable accessory, as illustrated in Fig. 1. This is intended to reduce the size and number of microcavities at the interface as well as subjecting a higher radial pressure than what the effect of the expanded SiR on the accessory alone would impose over longer period of time.[7] The external pressure must be adequate to ensure the necessary interfacial pressure; however, it should not induce permanent deformations to the materials involved. This approach increases the inception voltage of electrical discharges strongly enhancing the service reliability of the component.

Hence, the thermomechanical properties of SiR and the cable insulation need to be studied for designing better-performing cable terminations and connectors. Wu *et al.* investigated the effect of temperature cycling on SiR in tension from −40 to 90 °C and showed that hardness, elongation at break, and tensile strength increased with ageing time.[16] However, the behaviour of the same material under compression was not investigated. In another accelerated ageing study by Yu *et al.*, semiconductive SiR showed a decreasing shear modulus and an increasing surface roughness with ageing temperature and time in dry air.[12] Persson *et al.* assessed the stress relax-

ation behaviour of SiR under compression at 23 °C, and the rate of stress relaxation was observed to increase with higher strain amplitudes.[17] Only a few studies have examined SiR stress relaxation under compression together with additional factors such as temperature changes, as considered here.

The stress-relaxation behaviour of SiR may significantly contribute to the changes observed at a solid–solid polymer interface. Hence, studying the stress-relaxation behaviour of SiR under thermal and mechanical stresses is critical. In this work, we therefore investigated the effect of temperature cycling under compression on the properties of different grades of SiR materials used in HV cable accessories. In addition, cross-linked polyethylene (XLPE) samples were investigated as a reference for the cable insulation. Insulating SiR of different grades, semiconductive SiR and XLPE samples were subjected to accelerated ageing following ISO 3384-2:2019. Changes in material properties and a possible degradation mechanism due to accelerated ageing are discussed. The results will elucidate how these materials respond to thermal variations and external compressive pressure, providing insights essential for upgrading cable accessories to next-generation, higher-capacity, cost-effective designs.

2. Materials and methods

2.1. Materials investigated

Two types of insulating and one semiconductive SiR were manufactured in sheets by NKT GmbH Kabelgarnituren, Nordenham, Germany, and used as received. To fabricate XLPE plates, polyethylene pellets were extruded and subsequently cross-linked during casting to form plates of the specified dimensions. Cylindrical samples (29.0 ± 0.5 mm diameter, 6.3 ± 0.3 mm thickness) were punched from the plates using a waterjet for SiR and a metallic die for XLPE. The cut XLPE samples were then preconditioned for one week at 70 °C in vacuum.

2.2. Thermomechanical cycling procedure

The cylindrical samples were aged in a climate chamber following method B described in ISO 3384-2:2019.[18] For each sample category, a total of eight specimens were subjected to 336 h of thermal cycling, under two conditions: (i) without compression on a stainless-steel plate (4 specimens) and (ii) with constant compression to induce thermomechanical stress (4 specimens). For samples aged under thermomechanical stress, a constant 25% height reduction was applied using a custom-designed mechanical compression device, shown in Fig. 2. Height reduction refers to the percentage reduction in the original thickness of the sample with the help of two parallel compression plates. For a 25% height reduction, an originally 6.3 mm-thick sample was compressed to a gap thickness of 4.7 mm between the compression plates. The stainless-steel compression plates were polished to a roughness profile with an average roughness, R_a, of less than 0.4 μm. The type T thermocouple was placed close to the SiR or XLPE samples.
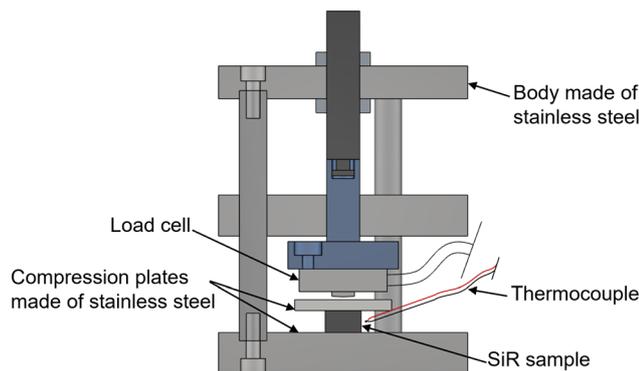
Fig. 2 Schematic illustration of the pressure device used during accelerated ageing. The 5 kN load cell connected to a data logger was used to measure the relaxation behaviour.

Both the thermocouple and the load cell were connected to a data logger (Agilent, Santa Clara, US) for continuous data recording. Changes in the counterforce during the temperature cycling were recorded by the standard force measured by a 5 kN load cell (Omega, Manchester, UK), which was used to measure the relaxation behaviour. Silicone oil (kinematic viscosity 50 mm^2 s^{-1}) was used as a lubricant between the samples and the compression plates to minimise friction effects.

The temperature profile shown for two cycles in Fig. 3 was used, and a total of 42 cycles were run. Included in Fig. 3 is also the recorded temperature close to the sample surface. Temperatures ranging from −20 to 110 °C were selected to assess material behaviour beyond the upper normal operation temperature, and rapid temperature cycling was done to induce thermal fatigue within the materials. Heating and cooling rates of 1.0 K min^{-1} were used, and a holding time of 2 h at the maximum and minimum temperatures was utilised
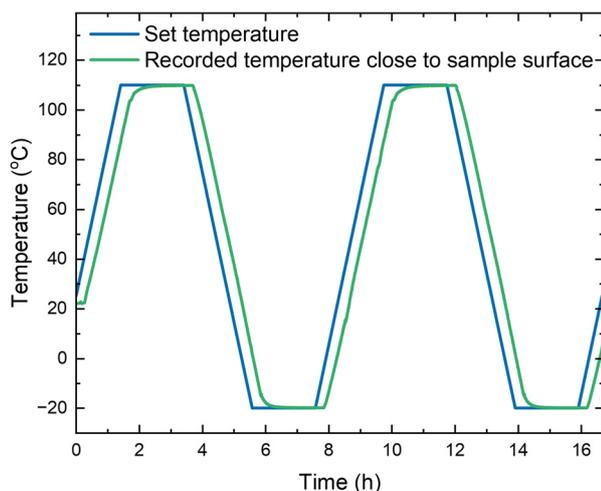

Fig. 3 Comparison between the set-temperature profile and the recorded temperature during the first two cycles of the thermomechanical testing.

to ensure homogenous temperature distribution within the samples.

2.3. Assessment of compression set and stress relaxation

The assessment of the compression set used to study the elastic recovery of unaged and aged materials was guided by ISO 815-1:2019.[19] Compression set refers to the permanent deformation that remains in a rubber material beyond its compression for a period of time after the compressive force is removed. A lower compression set corresponds to minimal change in interfacial pressure between materials on the component (cable accessory) over time, in addition to better sealing ability and elasticity which are vital for long-term performance. The compression set was calculated according to eqn (1):

$$\text{Compression set } (\%) = \frac{t_0 - t_f}{t_0 - t_s} \times 100 \qquad (1)$$

where t_0 is the initial thickness of the sample, t_s is the thickness under compression, and t_f is the final thickness of the sample after 30 min of recovery following the release of the 25% height reduction. The thicknesses were measured using a Digital ABS AOS Calliper (Mitutoyo Corporation, Kawasaki, Japan).

The stress relaxation over 24 h at 20 °C of unaged and accelerated aged samples was measured using the 5 kN load cell according to the procedure described in our previous work.[20] The samples were compressed to 25% height reduction, and the decline of the counterforce for 24 h was measured. The compression stress ratio was calculated using the expression, F_t/F_0, where F_0 is the maximum force measured by the load cell after 60 s of the application of the 25% height reduction and F_t is the force recorded continuously by the load cell over the entire duration of the investigation.

2.4. Analysis of cyclic loading

Repetitive compressive loads were applied to all material categories to assess the strain energy absorbed and released per unit volume in unaged and aged samples at ambient temperature. Height reductions in compression of 10, 25, 50, and 75% were applied. The analyses were performed using a UTS 200.4–200 kN universal testing machine (UTS Testsysteme, Ulm, Germany). A loading speed of 10 mm min^{-1}, which corresponds to a strain rate of 0.0278 s^{-1} for 6 mm thick samples, was employed. For each compressive strain category, a total of 5 cycles were conducted.

2.5. Morphology, thermal, and structural characterisation

The surface morphology of SiR and XLPE samples before and after accelerated ageing was examined on a JEOL – IT800 low vacuum (30 bar) field emission scanning electron microscope (SEM) (Joel, Akishima, Tokyo, Japan). Cross-sectional images were obtained under high vacuum using the hybrid lens mode at 1 kV. Sample cross-sections were cut with a scalpel and subsequently cleaned with ethanol before imaging.

The roughness of the sample surfaces before and after accelerated ageing was examined using a non-contact optical profilometer (Bruker Contour GT, Billerica, USA). A total of three scans were made at random positions on the top surface of samples from which the average values of roughness and standard deviation were obtained. Areal average surface roughness, S_a, was calculated by VISION 64 software, by averaging absolute values of surface height differences from a reference plane determined by the lowest point on the measured surface. Image processing involved using a "data restore" filter meant for interpolating missing data points to the raw data.[21]

Thermal stability of the materials up to 1000 °C was studied using thermogravimetric analysis (TGA) on a Netzsch – STA449 Jupiter TGA (Netzsch, Selb, Germany). Synthetic air and a heating rate of 10 K min^{-1} were used. Material hardness was assessed on a Shore A scale guided by ASTM D2240-15 using a digital durometer (SaluTron Messtechnik, Frechen, Germany). An average of ten measurements was reported. Phase transitions were assessed by differential scanning calorimetry (DSC) using a Netzsch – DSC Polyma 214 (Netzsch, Selb, Germany) using aluminium pans with a closed pierced lid. An initial heating to 200 °C was used, followed by cooling to −160 °C and then heating again to 200 °C. Infrared spectra were recorded using a Bruker Vertex 80v – FTIR spectrophotometer (Bruker, Billerica, US).

3. Results

3.1. Thermomechanical cycling

Sample categorisation was based on shore A hardness values, where hard SiR possessed an average hardness of 75, soft SiR a hardness value of 32, and semiconductive SiR (also named as semicon. SiR) at 41, as shown in Fig. S1 in SI. The force applied to each sample at the beginning and changes in the measured counterforce as each sample went through temperature cycling under the fixed height reduction of 25% are presented in Fig. 4. Similar repeated load cycling was observed for the four parallels of each material type studied. Due to the rubbery nature of SiR-based materials, they possessed a cyclic behaviour of expanding and contracting throughout the accelerated ageing, as shown in Fig. 4(a)–(c). The changes in the

measured standard force during the cyclic ageing can be attributed to the stress relaxation response to thermomechanical cycling. The XLPE reference samples showed a subtle recovery from the initial compression, as shown in Fig. 4(d) due to their characteristic plastic behaviour. All samples underwent an initial physical relaxation, as shown in Fig. S2, which presents the first two cycles. The last two cycles shown in Fig. S3 confirm that the SiR-based materials underwent a similar expansion and contraction throughout the ageing process.

3.2. Post-ageing compression set and stress relaxation analysis

A general increase in compression set was observed for the SiR-based samples after ageing under 25% compression, as shown in Fig. 5(a). The soft SiR showed a lower percentage increase in compression set than hard SiR. The stress relaxation effect was assessed by measuring the decline in the counterforce by the material and thereafter calculating the compression stress ratio at ambient temperature. The compression stress ratio after the accelerated ageing for samples assessed for 24 h is shown in Fig. 5(b)–(d). The compression stress ration was higher for the aged samples compared to the unaged for all types of materials. At 25% height reduction, the relaxation profile of hard SiR in Fig. 5(b) was steeper than for the profiles of soft SiR in Fig. 5(c) and semiconductive SiR in Fig. 5(d). In the early stages of the ageing, increased crosslinking of the SiR impedes the ability of the material to relax, hence decreased stress relaxation, however at longer ageing times, the rate of stress decay will increase due to chain scission giving the increased stress relaxation.

3.3. Cyclic loading assessment

Material response to cyclic loading for unaged and aged samples is shown in Fig. 6 and S4 at different height reductions. Increasing height reduction in compression was used to assess the effect of elevated compressive stress on the strain energy absorbed and released per unit volume. The resulting stress–strain behaviour was dependent on the maximum loading condition previously encountered for each sample. A typical Mullins (stress softening) effect was observed for both SiR-based and XLPE samples.[22]
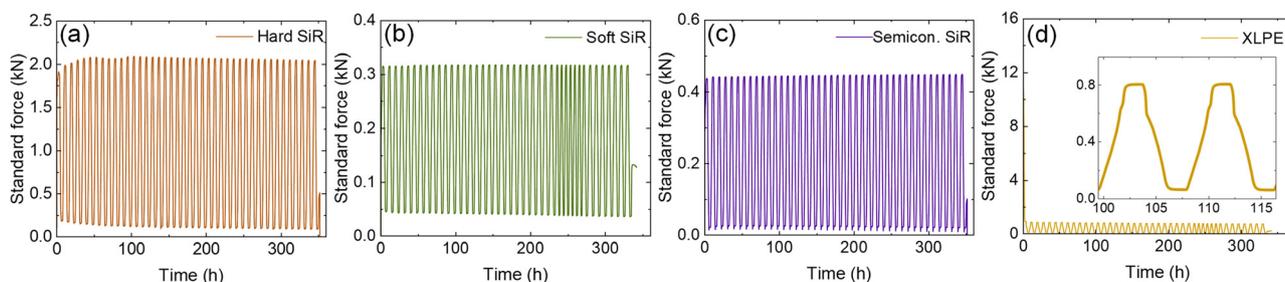

Fig. 4 Measured standard force *vs.* time for (a) hard SiR, (b) soft SiR, (c) semiconductive SiR and (d) XLPE samples during thermomechanical cycling between −20 and 110 °C at a holding time of 2 h both at the lowest and highest temperatures.
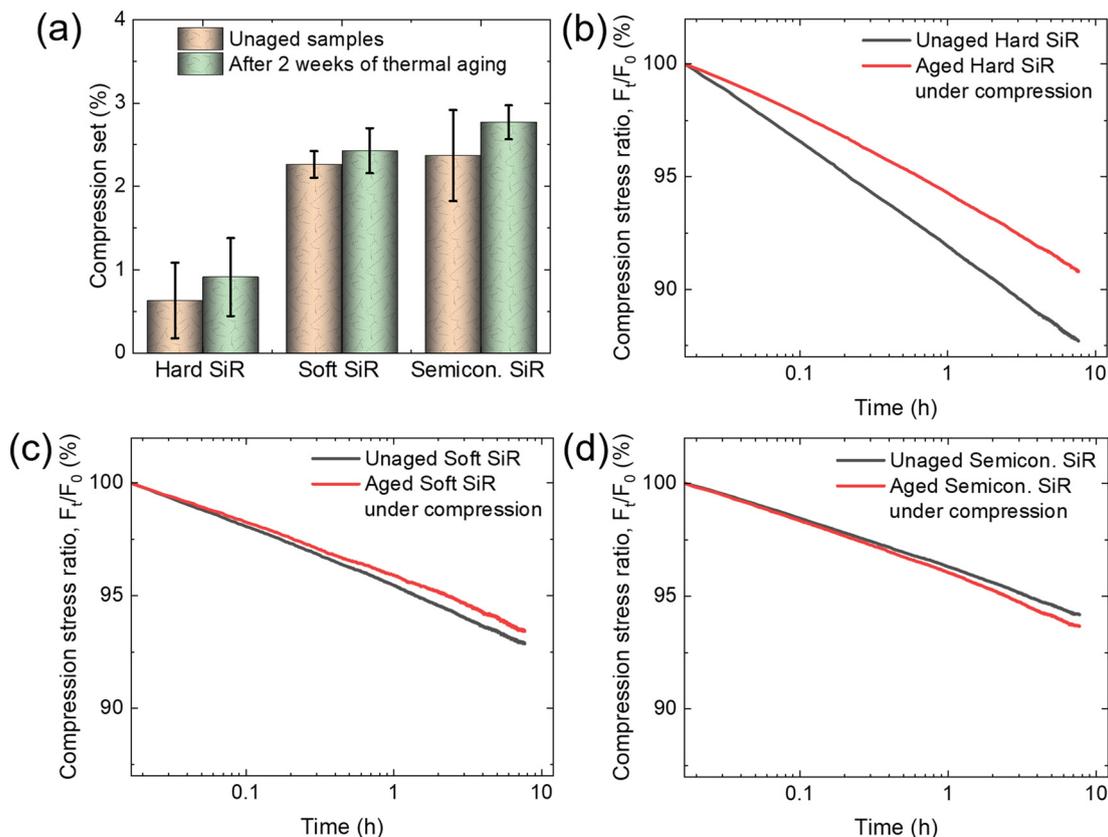
Fig. 5 (a) Compression set for SiR materials and material response to stress relaxation assessment prior to and after the accelerated ageing for (b) hard SiR, (c) soft SiR and (d) semiconductive SiR. The samples were kept under 25% compression for 24 h at ambient temperature.

For hard SiR and XLPE, the initial loading profile was different from consecutive loading profiles at a similar size reduction, which was not observed for soft and semiconductive SiR. For soft SiR, the consecutive loading profiles were similar to the respective initial loading profile showing that these materials recover from the deformation, especially at lower compression ratios. The change observed in hard SiR and XLPE can be attributed to higher energy dissipation during the initial loading and unloading cycles caused by irreversible structural changes in the materials.[23] Considering the last cycle of the highest height reduction (75%), the engineering stress *vs.* strain relationship showed different responses. As presented in Fig. 7, hard SiR endured a higher stress compared to semiconductive and soft SiR samples. However, XLPE endured the highest value of stress compared to the rubbery SiR materials.

The strain energy absorbed, released and energy dissipated per unit volume summarised in Table 1 detail material response shown in the last cycle of applying 75% strain. A higher strain energy was absorbed than released per unit volume. Materials aged under compression dissipated less strain energy during the cyclic loading to 75% height reduction. Since a larger surface area was exposed for samples aged without compression, significant structural changes in the polymer matrix could have been responsible for their altered mechanical behaviour. A reduction in strain energy dissipated was observed for the aged samples compared to the unaged irrespective of the sample type. The change in relative compression force *vs.* time for 5 cycles at 75% height reduction is presented in Fig. S5. A decline in the maximum compression force achieved at different repeated 75% height reductions was observed for hard SiR and XLPE while for soft and semiconductive SiR, an increase in the compression force was observed. For SiR samples, the compression force nearly appeared within the same loading time, but this was significantly different in XLPE samples as shown in Fig. S5 where there was a clear time difference.

3.4. Hardness

An increase in hardness was observed for all material types after the accelerated ageing. SiR-based materials aged without compression showed a stronger increase in hardness compared to those aged under compression, as shown in Fig. 8. However, for XLPE, a larger increase in hardness was observed for samples aged under compression. Hardness increases in aged materials corresponded with an observed increase in compression set with increasing ageing time, consistent with literature.[24,25] The increase in hardness can be linked to enhanced post-crosslinking and molecular interactions between the nanofillers and the SiR matrix in the early stages
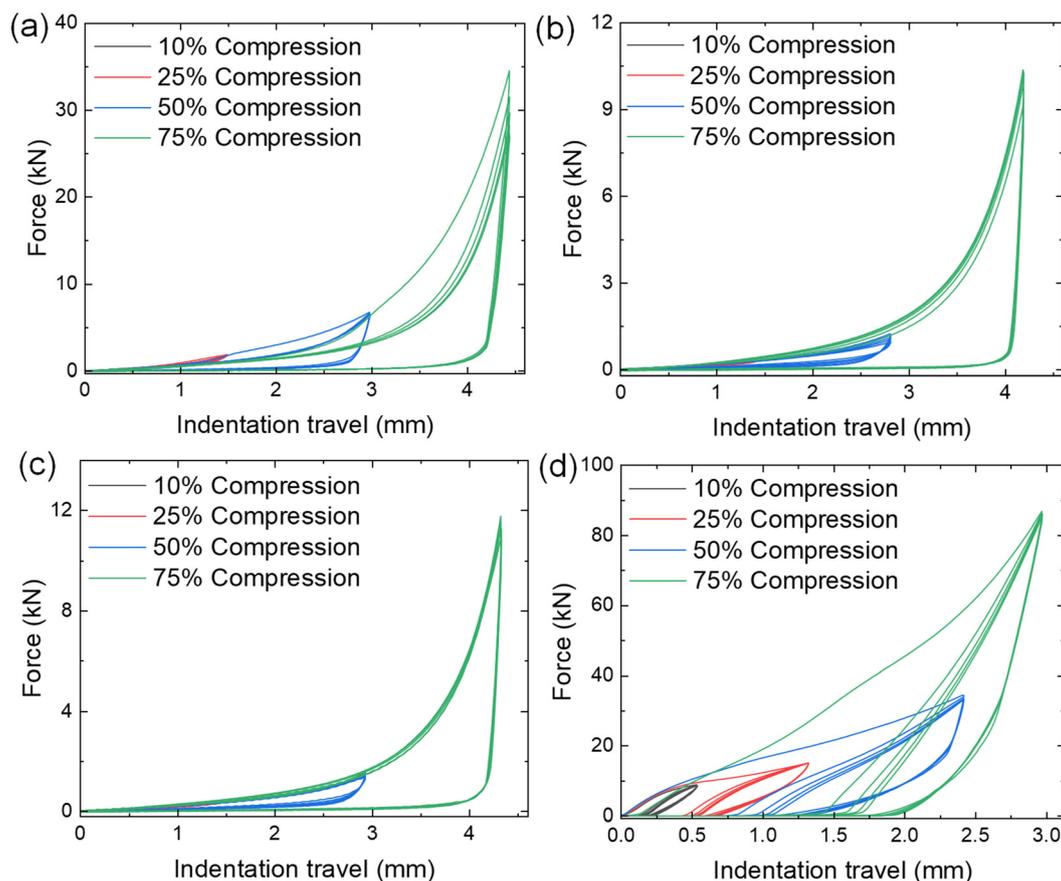
Fig. 6 Material response for aged samples under 25% compression to cyclic compression at different height reductions for (a) hard SiR, (b) soft SiR, (c) semiconductive SiR and (d) XLPE samples. A loading speed of 10 mm min^{-1} corresponding to strain rate of 0.0278 s^{-1} was used.

of the accelerated ageing process.[26] A significant change in sample mass and thickness was observed after the accelerated ageing, as shown in Fig. S6 and S7. The increase in mass of SiR-based samples under compression can be attributed to the diffusion of silicone oil, used as a lubricant, into the rubber matrix. A significant decrease in thickness was observed for the materials aged under compression (Fig. S7(b)).

3.5. Surface morphology

SEM images of unaged and aged SiR-based material surfaces presented in Fig. S8 show nearly the same morphology. However, there was an observable distinction on sample cross-sections as shown in Fig. 9. Cross section of SiR-based samples aged under and without compression had a rougher surface comprised of tiny particles. Similar features have previously been attributed to inorganic fillers separating out of the SiR rubber matrix.[12] The separation of additives from the material bulk of semiconductive SiR was enhanced by the ageing and was more prominent in the samples aged in a combination of thermal and mechanical stresses. Thermal cycling could have possibly weakened the bonding between the additives and the SiR, hence particles being observed on the cross-section of aged samples.

3.6. Surface roughness

Optical profilometry analysis of unaged and aged samples showed variation of surface roughness as presented in Table 2. An increase in average surface roughness was observed after ageing under compression for all sample categories and a reduction was observed for samples aged without compression. The contribution of the surface profile of compression plates to the roughness of aged samples was minimised by the application of silicone oil lubricant. For materials aged under compression a small increase in surface roughness was observed. Materials aged without compression were only subjected to thermal stress which could have induced realignment of molecular chains within the polymeric bulk and resulting in a reduced surface roughness.

3.7. Thermal properties

DSC data of the SiR-based and XLPE materials are presented in Fig. S9. The temperature range used for the thermomechanical cycling did not include any thermal events for the SiR-based materials. XLPE, however shows a thermal event in the upper temperature range (90 to 110 °C) due to partial crystallisation as has been previous reported.[27–29] The mass loss of the different materials during thermogravimetric analysis in syn-
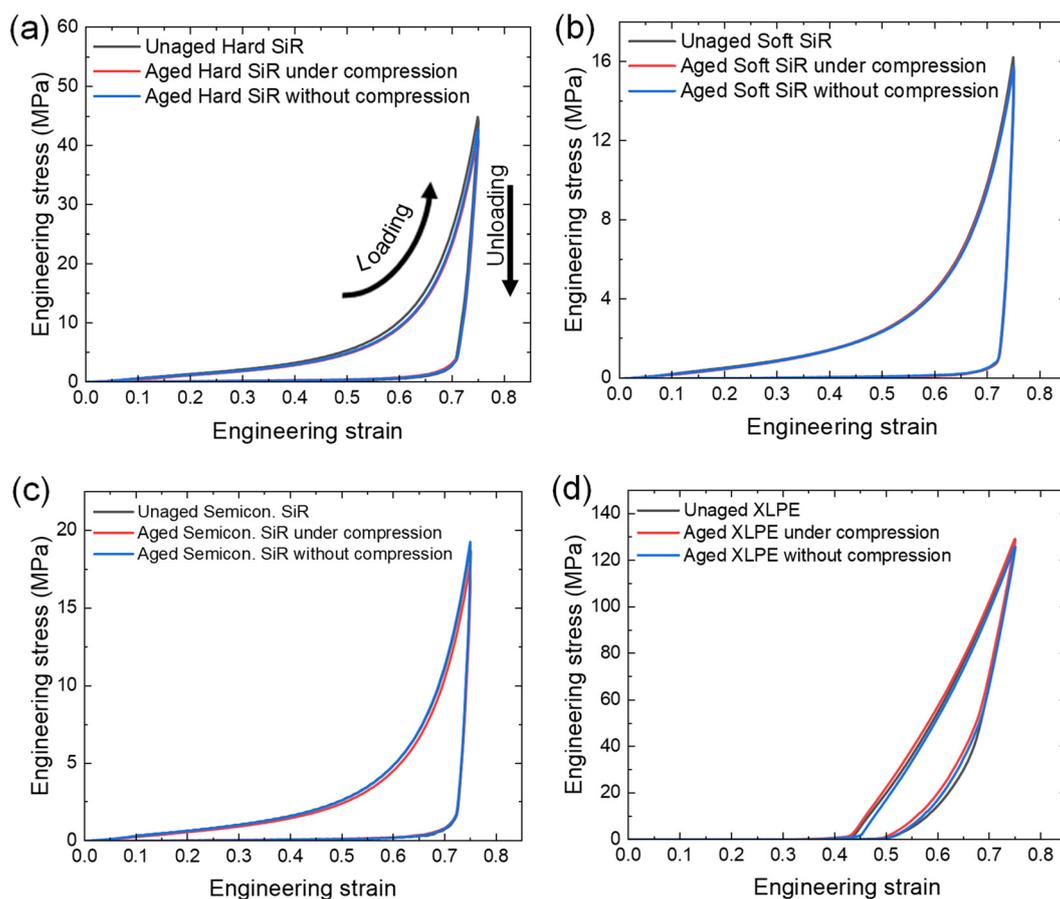
Fig. 7 Loading and unloading behaviour of (a) hard SiR, (b) soft SiR, (c) semiconductive SiR and (d) XLPE for the last cycle of 75% height reduction. A loading and unloading speed of 10 mm min^{-1} corresponding to strain rate of 0.0278 s^{-1} was used.

Table 1 Calculated strain energy and energy dissipated in the last cycle of 75% height reduction for unaged and aged SiR and XLPE samples

Sample type	Ageing process	Compression size reduction	Strain energy absorbed per unit volume (mJ mm^{-3})	Strain energy released per unit volume (mJ mm^{-3})	Energy dissipated per unit volume (mJ mm^{-3})
Hard SiR	Unaged	0%	5.1	1.0	4.1
	Aged	25%	4.6	1.0	3.6
		0%	4.7	1.0	3.7
Soft SiR	Unaged	0%	2.1	0.2	1.9
	Aged	25%	2.0	0.2	1.8
		0%	1.9	0.2	1.7
Semicon. SiR	Unaged	0%	2.3	0.3	2.0
	Aged	25%	2.1	0.3	1.8
		0%	2.3	0.3	2.0
XLPE	Unaged	0%	17.8	8.5	9.3
	Aged	25%	18.3	9.4	8.9
		0%	17.0	8.8	8.2

thetic air is provided in Fig. S10. The temperature range used for the accelerated ageing process was lower than the decomposition temperatures of the materials analysed.

The visual appearance of the samples before and after accelerated ageing is shown in Fig. S11. Unaged XLPE, hard and soft SiR possessed a translucent appearance whereas the aged samples turned yellowish. The yellowish effect was intense in XLPE as well as insulating SiR that were aged without compression. Since the thermomechanical cycling was performed in air, oxidation of the materials might occur. However, FTIR analysis of the materials (Fig. S12 and S13) did not show that significant oxidation had occurred. Minimal changes were observed for the bands at 714 and 720 cm^{-1}, indicating that there was limited oxidation to a carboxyl and
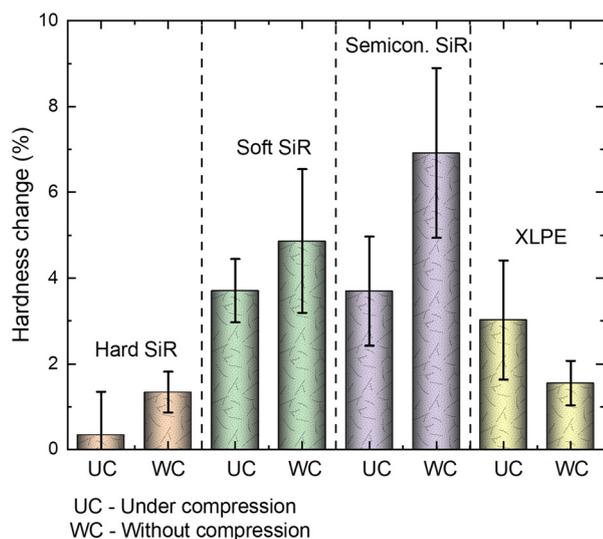
Fig. 8 Percentage change in hardness for all materials after being subjected to accelerated ageing.

ketone groups respectively, and this infers that the materials were resistant to oxidation during the accelerated ageing.

4. Discussion

Maintaining a high interfacial pressure between SiR and XLPE on a cable accessory is crucial, as it ensures a high AC breakdown strength of the cable accessory.[7–10] From the cyclic compression analysis after thermomechanical ageing obtained at ambient temperature (Fig. 6), soft SiR exhibited a lower stress relaxation response than hard SiR. Stress relaxation is in general induced by physical and chemical processes. While physical processes are favoured for short time periods and at ambient to low temperatures, chemical processes are favoured at extended time periods and at elevated temperatures.[30] The mobility of polymer chains highly influences the physical relaxation response. The observed stress relaxation which is most probably physical is in agreement with literature.[31,32] The observed Mullins effect (stress softening) was significantly dependent on the material type. More strain energy per unit
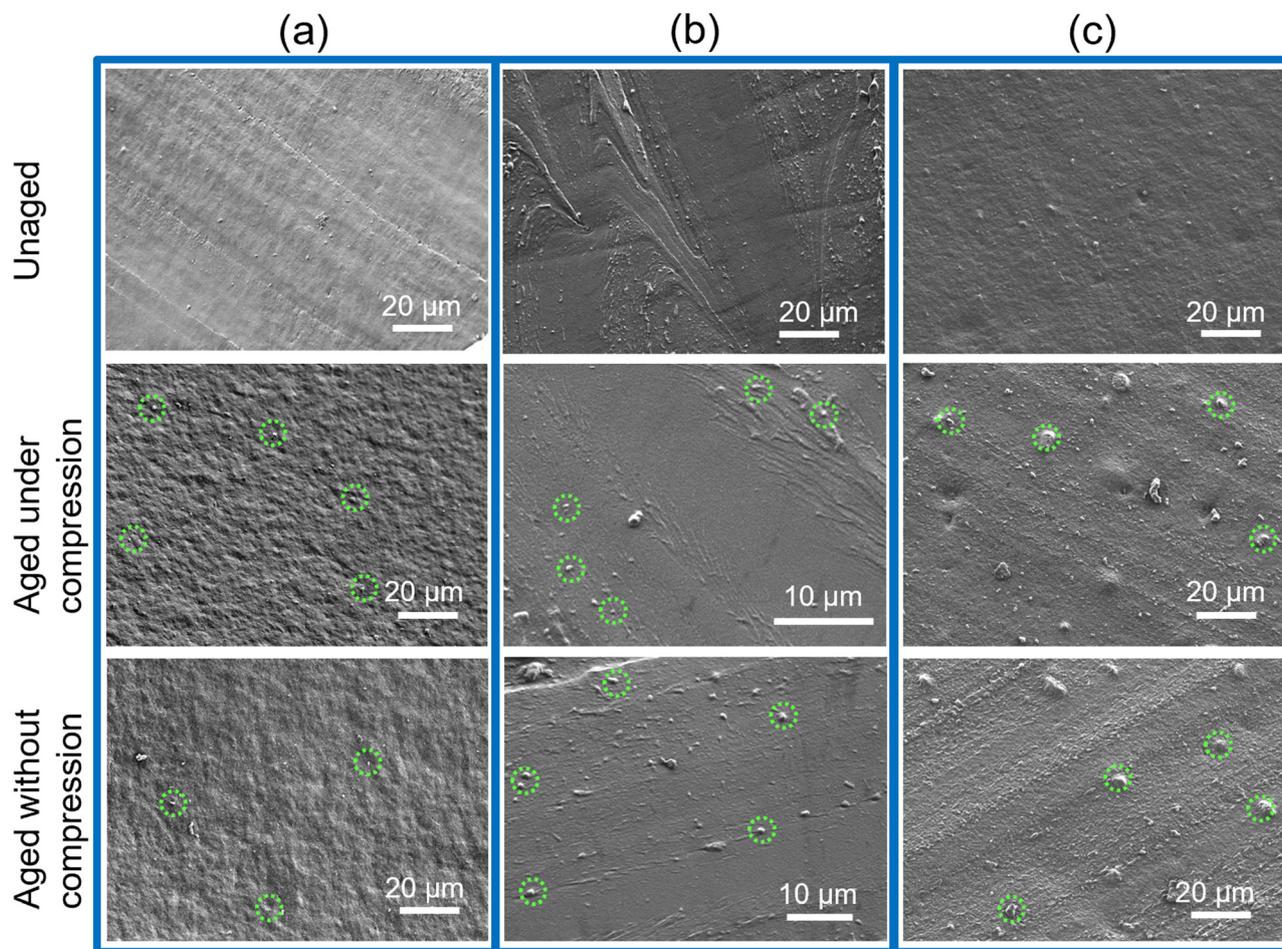

Fig. 9 SEM images of cross-sections of the bulk of unaged and aged (a) hard SiR (b) soft SiR and (c) semiconductive SiR materials. The dotted circles show inorganic solid particles on sample cross-sections.

Table 2 Areal average roughness, S_a calculated from surface profile images obtained from a non-contact optical profilometer

	Hard SiR		Soft SiR		Semicon. SiR		XLPE	
	S_a (µm)	SD	S_a (µm)	SD	S_a (µm)	SD	S_a (µm)	SD
Unaged	0.60	0.024	0.64	0.010	0.62	0.029	0.35	0.066
Aged under compression	0.66	0.079	0.86	0.066	0.70	0.254	0.47	0.012
Aged without compression	0.56	0.055	0.58	0.010	0.52	0.049	0.17	0.028

volume (Table 1) was dissipated in XLPE due to the plastic nature than in SiR-based materials. A clear difference in the strain energy absorbed in the first cycle was observed for the SiR-based materials (Fig. 6). For hard SiR, most of the softening appears after the first cycle and there is a distinct change of the loading curve for consecutive cycles.[22] For soft SiR, stress softening occurs along the loading curve of the initial cycle, with no significant difference in the amount of energy absorbed during loading for consecutive cycles. A similar behaviour was observed for semiconductive SiR. Moreover, under cyclic compressive stress, hard SiR absorbs more strain energy per unit volume than soft SiR. These results suggest that structural changes may have occurred in hard SiR as a result of the thermomechanical cycling, a response that was not observed in soft SiR. Significant changes in the mechanical properties of SiR are undesirable for the cable termination design illustrated in Fig. 1, as they can result in interfacial pressure loss. A lower stress relaxation response of SiR is desirable as it aids in retaining the required interfacial pressure.

The lower stress relaxation response for soft SiR compared to hard SiR when subjected to thermomechanical stresses is therefore beneficial for the modified cable termination design. In addition, semiconductive SiR possessed a different mechanical response, which, if altered to match that of soft SiR, would be a better combination for the modified cable termination design. Hence, soft SiR is a suitable candidate material for the modified HV cable accessory design applying an extended external pressure. This will facilitate maintenance of a sufficient interfacial pressure at the solid–solid interfaces, *i.e.*, between SiR and XLPE.

5. Conclusions

Accelerated ageing through combined thermal and mechanical stresses increased surface hardness, compression set, and roughness of SiR and XLPE materials used in HV cable accessories. Compared to unaged samples, aged materials exhibited reduced stress relaxation and diminished energy dissipation under cyclic loading, indicating a general decline in mechanical performance. Soft SiR demonstrated better suitability for cable terminations with external pressure devices due to its lower stress relaxation and minimal property degradation. Aligning the mechanical properties of semiconductive SiR with soft SiR will be emphasised in future work to prevent internal stress concentrations at cross-linked interfaces between insulating and semiconducting SiR and enable high

interfacial pressures between SiR and peeled XLPE cable surfaces.

Author contributions

OK: Data curation, formal analysis, investigation, methodology, validation, visualisation, writing – original draft; EK: Conceptualisation, formal analysis, funding acquisition, methodology, project administration, resources, supervision, validation, visualisation, writing – review & editing; SMH: Methodology, investigation, validation, writing – review & editing; JG: Supervision, validation, writing – review & editing; SH: Conceptualisation, funding acquisition, methodology, supervision, validation, writing – review & editing; MAE: Conceptualisation, formal analysis, methodology, supervision, validation, writing – review & editing.

Conflicts of interest

There are no conflicts to declare.

Data availability

Data for this article, including raw files from the different experiments are available at Zenodo (DOI: https://doi.org/10.5281/zenodo.18507412).

Selected data is included in the supplementary information (SI). Supplementary information is available. See DOI: https://doi.org/10.1039/d5lp00369e.

Acknowledgements

© 2026 The Author(s). Published by the Royal Society of Chemistry

RSC Appl. Polym., 2026, **4**, 785–795 | **793**

References

1 Y. T. Li, W. J. Liu, F. X. Shen, G. D. Zhang, L. X. Gong, L. Zhao, P. Song, J. F. Gao and L. C. Tang, Processing, thermal conductivity and flame retardant properties of silicone rubber filled with different geometries of thermally conductive fillers: A comparative study, *Composites, Part B*, 2022, **238**, 109907.

2 M. Chen, Y. Wang and Y. Yin, Dielectric Strength and Failure Mechanism of Power Module Packaging Insulation at Ultra-High Temperature, *Proc. Int. Symp. Electr. Insul. Mater.*, 2023, 243–246.

3 M. Zare, M. Ehsani, A. A. Shayegani Akmal, R. Khajavi and D. Zaarei, Development of silicone rubber-based nano-composites: nanoparticle selection and performance analysis, *Polym. Technol. Mater.*, 2024, **63**, 399–418.

4 D. Fournier, Effect of the surface roughness on interfacial breakdown between two dielectric surfaces, *IEEE Int. Symp. Electr. Insul.*, 1996, 699–702.

5 D. Fournier and L. Lamarre, Effect of pressure and length on interfacial breakdown between two dielectric surfaces, *Conf. Rec. IEEE Int. Symp. Electr. Insul.*, 1992, 1992-June, 270–272.

6 E. Kantar and S. Hvidsten, A deterministic breakdown model for dielectric interfaces subjected to tangential electric field, *J. Phys. D: Appl. Phys.*, 2021, **54**, 1–19.

7 E. Kantar, S. Hvidsten and J. Aakervik, Effect of Radial Pressure and Lubricant Types on Partial Discharge Inception in a Slip/On Medium Voltage XLPE Cable Termination, *Jicable'23 – 11th Int. Conf. Power Insul. Cables, Lyon – Fr.*, 2023, 1–6.

8 E. Kantar, E. Ildstad and S. Hvidsten, Effect of elastic modulus on the tangential AC breakdown strength of polymer interfaces, *IEEE Trans. Dielectr. Electr. Insul.*, 2019, **26**, 211–219.

9 C. Dang and D. Fournier, Dielectric performance of interfaces in premolded cable joints, *IEEE Power Eng. Rev.*, 1997, **17**, 36–37.

10 K. Temmen, Evaluation of surface changes in flat cavities due to ageing by means of phase-angle resolved partial discharge measurement, *J. Phys. D: Appl. Phys.*, 2000, **33**, 603–608.

11 International Electrotechnical Commission, Iec 60502-1:2021, 2021, 3.0, 1–8.

12 J. Yu, Z. Zhang, W. Ren, D. Yang, D. Wu, Z. Ning, C. Fang and J. Wu, Aging Analysis of Semiconductive Silicone Rubber for 10 kV Cold-Shrink Cable Accessories, *Energies*, 2024, **17**, 1–18.

13 B. X. Du, Y. Zhang, T. Han and Z. L. Li, Temperature Gradient Affecting Electrical Tree in Silicone Rubber under Impulse Superimposed on DC Voltage, *IEEE Trans. Dielectr. Electr. Insul.*, 2021, **28**, 1480–1487.

14 Y. H. Wei, H. Guo, X. L. Chen, X. J. Li, G. C. Li, Y. Nie and Y. W. Zhu, Compression stress relaxation characteristics and failure mechanism of silicone rubber for high voltage cable accessories, *Polym. Degrad. Stab.*, 2025, **231**, 111098.

15 S. Zierhut, T. Klein, E. Wendt and Z. Lutz, Influence of expansion on electric field distribution of stress cones for high voltage cable accessories, *Jicable'15 – 9th Int. Conf. Insul. Power Cables, Versailles* 21–25 *June* 2015, 2015, 15–21.

16 C. Wu, Z. Miao, X. Wang, Y. Zhang, Z. Chen and Y. Yang, The Effect of High-low Temperature Cycle Ageing on Mechanical Properties of Silicone Rubber under Tensile State, 2023 *IEEE 4th Int. Conf. Electr. Mater. Power Equipment, ICEMPE* 2023, 2023, 1–4.

17 A. M. M. R. Persson and E. Andreassen, Cyclic Compression Testing of Three Elastomer Types— A Thermoplastic Vulcanizate Elastomer, a Liquid Silicone Rubber and Two Ethylene-Propylene-Diene Rubbers, *Polymers*, 2022, **14**, 1–32.

18 ISO, Rubber, vulcanized or thermoplastic—Determination of stress relaxation in compression—Part 2: Testing with temperature cycling, 2019, 3384–2, 1–22.

19 ISO, Rubber, vulcanized or thermoplastic—Determination of compression set—Part 1: At ambient or elevated temperatures, 2019, 815–1, 1–20.

20 O. Kayanja, E. Kantar, S. M. Helleso, S. Hvidsten, J. Glaum and M. A. Einarsrud, Effect of cyclic mechanical stress on the material properties of silicone rubber for HV subsea cable applications, in 2024 *IEEE International Conference on High Voltage Engineering and Applications, ICHVE* 2024 – *Proceedings*, IEEE, 2024, vol. 1, pp. 1–4.

21 E. Kantar, K. K. Eie-Klusmeier, T. A. Ve, M. H. Ese and S. Hvidsten, Electrical aging of fluoropolymer cable insulation materials induced by partial discharge, *IEEE Trans. Dielectr. Electr. Insul.*, 2024, **32**, 1–11.

22 J. Diani, B. Fayolle and P. Gilormini, A review on the Mullins effect, *Eur. Polym. J.*, 2009, **45**, 601–612.

23 T. T. Yang, Y. Shui, C. S. Wei, L. Z. Huang, C. W. Yang, G. A. Sun, J. J. Han, J. Z. Xu, Z. M. Li and D. Liu, Effect of cyclic straining with various rates on stress softening/hysteresis and structural evolution of filled rubber: A time-resolved SANS study, *Composites, Part B*, 2022, **242**, 110100.

24 R. Y. Wang, C. H. Wang, Y. Wang and W. F. Zhang, Synergistic Effects of Multiple Environmental Factors on Degradation of Silicone Rubber Seals under Marine Atmosphere, *Materials*, 2023, **16**, 1–17.

25 S. Li, Y. Ke, L. Xie, Z. Zhao, X. Huang, Y. Wang and Z. Wang, Study on the aging of three typical rubber materials under high- and low-temperature cyclic environment, *e-Polymers*, 2023, **23**, 1–14.

26 M. Akbar, R. Ullah and I. Qazi, Multi-stress aging investigations of HTV silicone rubber filled with Silica/ATH composites for HVAC and HVDC transmission, *Eng. Failure Anal.*, 2020, **110**, 104449.

27 C. Blivet, J. F. Larché, Y. Israëli, P. O. Bussière and J. L. Gardette, Thermal oxidation of cross-linked PE and EPR used as insulation materials: Multi-scale correlation over a wide range of temperatures, *Polym. Test.*, 2021, **93**, 1–10.

28 L. Boukezzi, A. Boubakeur, C. Laurent and M. Lallouani, DSC study of artificial thermal aging of XLPE insulation cables, 2007 *Int. Conf. Solid Dielectr. ICSD*, 2007, 146–149.

29 Z. Yang, H. Peng, W. Wang and T. Liu, Oxidation and Crosslinking Processes During Thermal Aging of Low-Density Polyethylene Films, *J. Appl. Polym. Sci.*, 2011, 5200–5208.

30 M. Zaghdoudi, A. Kömmling, M. Jaunich and D. Wolff, Erroneous or arrhenius: A degradation rate-based model for EPDM during homogeneous ageing, *Polymers*, 2020, **12**(9), 2152.

31 A. Pannikottu, C. Lu and M. Centea, Continuous Compression Stress Relaxation of Rubber Materials: Testing and Simulation, in *3rd International Symposium on Finite Element Analysis of Rubber and Rubber-Like Materials*, 1999, pp. 1–17.

32 S. Ronan, T. Alshuth, S. Jerrams and N. Murphy, Long-term stress relaxation prediction for elastomers using the time-temperature superposition method, *Mater. Des.*, 2007, **28**, 1513–1523.

© 2026 The Author(s). Published by the Royal Society of Chemistry

RSC Appl. Polym., 2026, **4**, 785–795 | **795**